

Communication

# Effects of His-Tag Length on the Soluble Expression and Selective Immobilization of D-Amino Acid Oxidase from *Trigonopsis variabilis*: A Preliminary Study

Zhipeng Yan <sup>1,†</sup>, Qinhe Zhu <sup>1,†</sup>, Li Ma <sup>2,†</sup>, Guihui Li <sup>1</sup>, Erzheng Su <sup>3</sup> , Jia Zeng <sup>1</sup>, Yongzhong Chen <sup>2</sup>, Er Meng <sup>1,\*</sup> and Senwen Deng <sup>1,2,\*</sup>

- <sup>1</sup> Hunan Key Laboratory of Economic Crops Genetic Improvement and Integrated Utilization, School of Life and Health Sciences, Hunan University of Science and Technology, Xiangtan 411201, China
- <sup>2</sup> National Engineering Research Center of Oiltea Camellia, Research Institute of Oiltea Camellia, Hunan Academy of Forestry, Shao Shan South Road, No. 658, Changsha 410004, China
- <sup>3</sup> Enzyme and Fermentation Technology Laboratory, College of Light Industry and Food Engineering, Nanjing Forestry University, Nanjing 210037, China
- \* Correspondence: menger@hnust.edu.cn (E.M.); dswwzls@hnust.edu.cn (S.D.)
- † These authors contributed equally to this work.

**Abstract:** His-tags are widely used for the purification of recombinant proteins. High-cost carriers functionalized with nickel ions are commonly required for the selective immobilization of His-tagged enzymes. In this study, His-tags of varying lengths were fused to the N-terminus of D-amino acid oxidase (DAO) from *Trigonopsis variabilis*. The attachment of a His6 tag significantly improved the solubility of the recombinant DAO expressed in *Escherichia coli*. By modulating the tag lengths, a better balance between cell growth and protein solubility was achieved, resulting in a higher volume activity (His3). Furthermore, the fusion of longer tags (His6 and His9) facilitated the rapid immobilization of DAOs onto a commercial epoxy carrier without metal bearing, resulting in more selective immobilization. In conclusion, the modulation of His-tag length was preliminarily demonstrated as a simple and cost-effective approach to achieve efficient expression, as well as fast and selective immobilization of DAO.

**Keywords:** His-tags; recombinant expression; immobilization; D-amino acid oxidase



**Citation:** Yan, Z.; Zhu, Q.; Ma, L.; Li, G.; Su, E.; Zeng, J.; Chen, Y.; Meng, E.; Deng, S. Effects of His-Tag Length on the Soluble Expression and Selective Immobilization of D-Amino Acid Oxidase from *Trigonopsis variabilis*: A Preliminary Study. *Processes* **2023**, *11*, 1588. <https://doi.org/10.3390/pr11061588>

Academic Editors: Hui Li and Yunting Liu

Received: 22 April 2023  
Revised: 12 May 2023  
Accepted: 16 May 2023  
Published: 23 May 2023



**Copyright:** © 2023 by the authors. Licensee MDPI, Basel, Switzerland. This article is an open access article distributed under the terms and conditions of the Creative Commons Attribution (CC BY) license (<https://creativecommons.org/licenses/by/4.0/>).

## 1. Introduction

His-tags are commonly used for the efficient purification of recombinant proteins via metal affinity chromatography [1–3]. They are routinely attached to the terminus of proteins, with the assumption that the fusion will not significantly affect the structure and function of the target proteins due to their small molecular weight [3]. The fusion position of His-tags can be varied to improve protein expression and purification [3–6]. D-amino acid oxidase (DAO) (E.C.1.4.3.3) is an important industrial enzyme, but its recombinant expression in *Escherichia coli* has been hindered by its low solubility and cytotoxicity [5]. N-terminal His-tag was found to improve the soluble and active expression of DAO from *Trigonopsis variabilis* in *E. coli*, while its C-terminus analogue did not [5]. Optimal His-tag length is crucial for the efficient expression and purification of specific proteins [7–10], while its effects on protein immobilization are less discussed.

In order to enhance the economy and controllability of biocatalytic processes, enzymes are often immobilized on carriers to facilitate the separation of products and the recycling of expensive biocatalysts [11–13]. Multiple-point covalent immobilizations are widely employed with various advantages, such as high stability [14]. However, the immobilization of enzymes on commonly used epoxy-based carriers can be time-consuming and unselective, leading to undesirable side reactions catalyzed by contaminating enzymes [15,16]. Additionally, purification processes of enzymes are often tedious and time-consuming. To

achieve one-step immobilization–purification of enzymes, heterofunctional supports have been developed. The selective immobilization of His-tagged enzymes can be achieved with heterofunctional supports containing metal ions [17]; however, the cost of these supports is considerably higher than the beads typically used for immobilization in the industry [18,19]. Thus, it is important to establish a time-saving and cost-effective strategy for the selective immobilization of enzymes.

In this study, the effects of His-tag lengths on the expression of DAO from *Trigonopsis variabilis* were first studied. Then, His-tagged DAOs were immobilized on epoxy-based carriers to study their effects on protein immobilization (Figure 1).

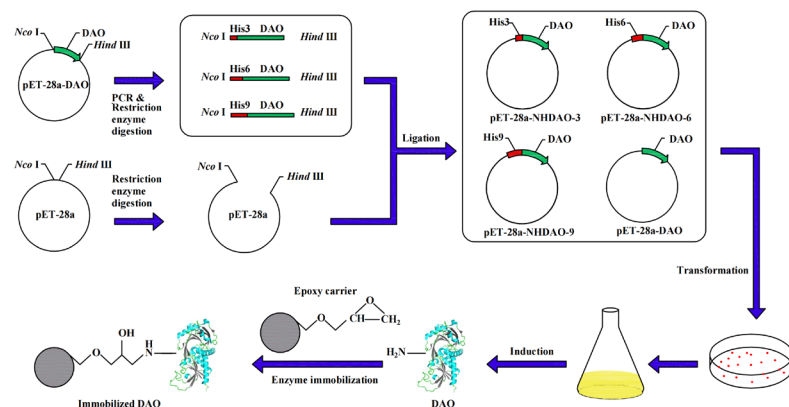


**Figure 1.** Graphical scheme of the expression and immobilization of His-tagged DAOs.

## 2. Material and Methods

### 2.1. Materials

Isopropyl- $\beta$ -D-thiogalactopyranoside (IPTG), D-alanine, and pyruvate were purchased from Sigma (St. Louis, MO, USA). Protein marker and T4 DNA ligase were bought from Thermo Fisher Scientific Inc. (Shanghai, China). KOD-plus DNA polymerase was bought from Toyobo Biotechnology Co., Ltd. (Shanghai, China). The Plasmid Mini kit, gel extraction kit, and synthesized oligonucleotides were obtained from Sangon Company (Shanghai, China). Restriction enzymes came from Solarbio Biotechnology Co., Ltd. (Beijing, China). Epoxy carrier (LX-1000EP, LX-103B) and amino carrier LX-1000EA were kindly provided by the Lanxiao Company (Shanxi, China).

### 2.2. Construction of Fusion Genes

DAO was fused with His-tags of different lengths using the PCR method with the plasmid pET-DAO as the template. The plasmids pET-DAO and pET-NHDAO-6 (D-amino acid oxidase fused with N-terminal His6 tag) were reserved in this lab [5]. The forward primers N-HIS-3 and N-HIS-9 with *NcoI* restriction site, and the reverse primer DAO-R with *HindIII* restriction site were used for the amplification of the fusion genes, abbreviated as NHDAO-3 (D-amino acid oxidase fused with N-terminal His3 tag) and NHDAO-9 (D-amino acid oxidase fused with N-terminal His9 tag), respectively. Their nucleoside sequences are as follows: N-HIS-3, 5'-CATGCCATGGCTCACCATCACAAAATCGTTGTTATTGGTGCCG-3'; N-HIS-9, 5'-CATGCCATGGCTCACCATCACCATCACCATCACCATAAAATCGTTGTTATTGGTGCCG-3'; and DAO-R, 5'-CCCAAGCTTCTAAAGGTTTGGACG-3'. Each PCR consisted of 25 cycles at 94 °C for 0.5 min, 55 °C for 0.5 min, and 68 °C for 1.1 min, using KOD-plus DNA polymerase. The PCR products and the vector pET-28a were digested with *NcoI* and *HindIII*, purified using a gel extraction kit, fused by T4 DNA ligase, and then transformed into *E. coli* DH5 $\alpha$ . The fused plasmids were extracted and sequenced. The correct plasmids were then transformed into *E. coli* BL21(DE3).

### 2.3. Cultivation Conditions of Recombinant DAOs

Single clones on Lysogeny Broth (LB) agar plates were inoculated into an LB medium containing 0.025 g/L of kanamycin. The seed cultures were shaking overnight at 37 °C and 200 rpm. Subsequently, 1.0% (*v/v*) of seed culture was inoculated into a flask containing 50 mL of LB medium. Cells were cultivated at 37 °C and 200 rpm until the optical density at 600 nm ( $OD_{600}$ ) reached 0.8–1.0, and 0.1 mM of IPTG was added to induce recombinant protein expression. After shaking at 20 °C and 200 rpm for 20 h, the cells were harvested via centrifugation at  $7378 \times g$  for 10 min and then washed twice with 100 mM of phosphate-buffered saline (PBS) at a pH of 7.8.

### 2.4. Crude Enzyme Preparation

The cell pellets were resuspended in freshly prepared 100 mM of PBS buffer (pH 7.8) and lysed using ultrasonic disruption in an ice-water bath (400 W, 99 cycles, working for 3 s with an interval of 5 s as one cycle). The supernatants were collected via centrifugation at  $11,644 \times g$  and 4 °C for 20 min. The supernatant and resuspended precipitation were analyzed using sodium dodecyl sulfate–polyacrylamide gel electrophoresis (SDS-PAGE). The protein content was determined based on the Bradford method [20]. Enzyme activity was determined by measuring the formation of pyruvate product [5]. One unit of enzyme activity was defined as the amount of enzyme that produced 1.0  $\mu\text{mol}$  of pyruvate per min. Specific activity was denoted as unit/mg protein of the sample.

### 2.5. Enzyme Immobilization

The immobilization process was conducted as described before [12,13,21]. The solution contained 1 M of PBS (pH 8.5), 20 g of epoxy carrier (LX-1000EP), and 700 mg of crude enzyme in a total volume of 200 mL. The samples were collected at indicated time points via centrifugation. The immobilized enzymes were resuspended in fresh PBS and shaken vigorously for 3 min before being collected again via centrifugation. This procedure was repeated three times to ensure that any enzymes not bonded covalently to the carriers were properly washed away. The activity and the protein concentration of the supernatants at different time points were measured. The ratio of residual activity = (total activity of supernatant/total activity of free enzymes solution used for immobilization)  $\times$  100%. The ratio of activity recovery = (total activity of immobilized enzyme/total activity of free enzymes solution used for immobilization)  $\times$  100%.

### 2.6. Protein Structure Homology Modeling

Protein structure homology modeling of DAO and NHDAO-6 from *Trigonopsis variabilis* was conducted using the I-TASSER server "<http://zhanglab.ccmb.med.umich.edu/I-TASSER> (accessed on 6 May 2023)" [22]. Given the species origin and catalytic property, the crystal structure (pdb ID:1C0P) of DAO from *Rhodotorula toruloides* (RgDAO) with a high resolution of 1.2 Å was chosen as the template. RgDAO is also widely used in the industry and frequently employed as a template for investigating the structure of DAO from *Trigonopsis variabilis* with a sequence identity of 31.19% [23]. Structural models were visualized using the PyMOL v2.3.1 software (The PyMOL Molecular Graphics System, Version 2.0 Schrödinger, LLC, New York, NY, USA).

## 3. Results and Discussion

### 3.1. Effect of His-Tag Lengths on Protein Expression

His-tags of varying lengths were added to the N-terminus of DAO via PCR, resulting in NHDAO-3, NHDAO-6, and NHDAO-9 (Figure 1). The impact of His-tag lengths on enzyme expression was analyzed through activity assay and SDS-PAGE analysis.

#### 3.1.1. Effect of His-Tag Lengths on Host Cell Growth

The impact of these His-tags on cell growth was found to be significant. In comparison to the untagged DAO, the cell density of the strain expressing NHDAO-6 was notably

lower. The cell densities of NHDAO-3, NHDAO-6, and NHDAO-9 were 4.04, 2.62, and 5.32 ( $OD_{600}$ ), respectively, which were 75.37%, 48.88%, and 99.25% of the cell density observed for DAO (Figure 2a). Recombinant expression of DAO in *E. coli* is usually hindered by its cytotoxicity since DAO catalyzes the degradation of D-Ala and D-Glu, which are important components of peptidoglycan [5].

### 3.1.2. Effect of His-Tag Lengths on Protein Solubility

To assess the effect of His-tag lengths on protein solubility, an SDS-PAGE analysis was conducted. It was observed that the solubility of DAO initially increased with the length of the His-tag. NHDAO-6 was expressed as a soluble protein, whereas a significant portion of DAO or NHDAO-9 was found in the form of inclusion bodies (Figure 2b). Whether this could be ascribed to the special folding/unfolding patterns or other factors remains uncertain. A previously reported T15A mutant DAO, where an alanine (Ala) substitution was introduced at the 15th amino acid residue, exhibited considerably lower solubility compared to the wild-type DAO [5]. These results suggest that the N-terminus is crucial for the correct folding of DAO.

### 3.1.3. Effect of His-Tag Lengths on Enzyme Activity

The high solubility of NHDAO-6 can lead to increased toxicity in the host cell, resulting in reduced biomass. Therefore, the total and specific activities of the NHDAO-6-bearing strain were not the highest. This could be alleviated by the addition of extra carbon source and the implementation of dissolved oxygen control during the fermentation process [5,24]. The highest total and specific activities were observed with the NHDAO-3-bearing strain (Figure 2a), which could be attributed to the balance between cell growth and protein solubility, although a large portion of NHDAO-3 was in the form of inclusion bodies. Consequently, modulating the lengths of His-tags presents a promising approach to enhance DAO production.

Soluble expression of industrial proteins is important for cost control. Various tags have been employed to improve the soluble expression of recombinant proteins, and our results suggest that the specific length of the tag used may serve as an additional contributing factor [25]. It is worth noting that these results are obtained at a flask scale, and the best recombinant strain should be chosen via fermentation experiments in a fermentor.

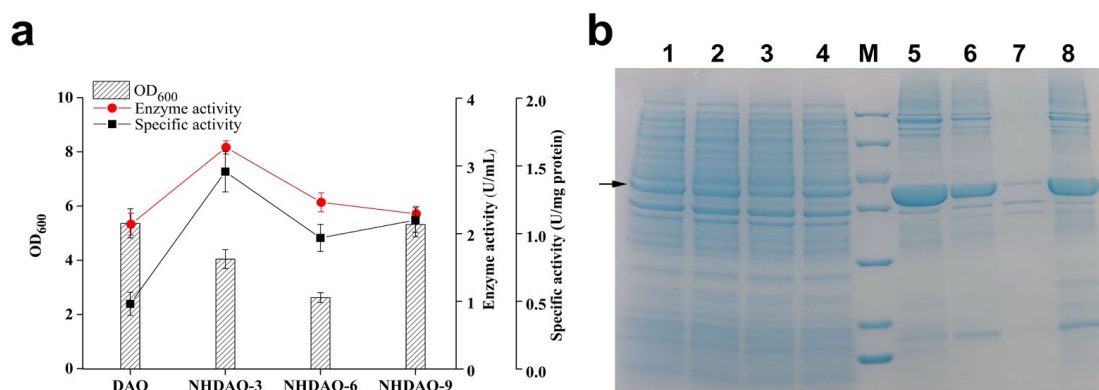


**Figure 2.** Effects of His-tag lengths on protein production. (a) Cell density, total activity, and specific activity of recombinant strains. The error bars represent the standard deviations (SDs) of three independent cultures of the same construct. (b) Solubility of DAOs fused with His-tags of different lengths. Lanes 1, 2, 3, and 4 are the soluble fractions of DAO, NHDAO-3, NHDAO-6, and NHDAO-9, respectively; Lanes 5, 6, 7, and 8 are the insoluble fractions of DAO, NHDAO-3, NHDAO-6, and NHDAO-9, respectively. Lane M: protein molecular marker of, from top to bottom, 116, 66.2, 45, 35, 25, 18.4, and 14.4 kDa. The arrow indicates the bands corresponding to DAOs.

### 3.2. Effect of His-Tag Lengths on Enzyme Immobilization

To explore the effect of His-tag lengths on enzyme immobilization, the crude enzymes of His-tagged DAOs were immobilized to the commonly used epoxy carrier LX-1000EP under the same condition.

#### 3.2.1. Effect of His-Tag Lengths on Immobilization Rate

The residual activities of DAOs in the immobilized solution were measured at different time points. The alteration in residual activities varied among the constructs. After 6 h of immobilization, the residual activities of DAO, NHDAO-3, NHDAO-6, and NHDAO-9 were 37.47%, 46.55%, 7.23%, and 0.17%, respectively (Figure 3a). These results indicated that the immobilization rate of DAO increased with the length of His-tag.

#### 3.2.2. Effect of His-Tag Lengths on Immobilization Selectivity

Moreover, the specific activities of NHDAO-9 and NHDAO-6 in liquid decreased during the immobilization process, while the values of NHDAO-3 and DAO remained nearly constant (Figure 3b). This was further confirmed by the SDS-PAGE analysis (Figure 3c). The bands corresponding to NHDAO-9 could hardly be observed after 6 h of immobilization, whereas the bands of DAO were still clearly visible at 12 h, suggesting that NHDAO-9 was selectively adsorbed onto the epoxy carrier.

#### 3.2.3. Effect of His-Tag Lengths on Immobilization Yield

The activity recovery of immobilized NHDAO-9 at 6 h was 37.24%, which was much higher than the value of 9.29% of DAO (Figure 3d). The activity recovery of NHDAO-9 did not increase at 12 h, while the activity recovery of DAO at 12 h increased to 16.89%, suggesting that most of NHDAO-9 were immobilized to the carrier at 6 h. These results indicated that the immobilization rates of DAOs fused with longer His-tags were much faster than those of untagged DAOs and host proteins, thus contributing to the selective immobilization of DAOs [26]. The fast and selective immobilization of NHDAO-9 was further confirmed using the epoxy carrier LX-103B and the amino carrier LX-1000EA from the same company (unpublished results).

#### 3.2.4. Effect of His-Tag Lengths on Protein Structure

It has been shown that His-tag fusion does not significantly affect the overall structure of DAO obtained through homologous modeling. However, the shallow buried N-terminal amide can be pushed out by His-tags with certain lengths (Figure 3e). The N-terminal amide, with a pKa < 7.5, is deemed one of the most active groups during the reaction with an epoxy resin [27]. The addition of His-tag might reduce the steric hindrance of N-terminal amide, facilitating its reaction with the epoxy resin. However, it is not clear whether His-tag fusion can change the orientation of enzyme immobilization or not.

Epoxy carriers are widely used in biocatalysis due to their excellent adsorption capacity and stability, but the immobilization processes at room temperature are often time-consuming (>24 h), which is unfavorable for the immobilization of unstable proteins [11–13]. Single-step purification and immobilization of His-tagged proteins have been previously studied using surfaces functionalized with nickel (II) ions; however, the cost of these immobilization carriers is relatively higher [18,19]. Selective immobilization of His-tagged proteins on commercial carriers can be more ideal for cost control. It is generally accepted that His-tag has minimal or no effect on the biological structure of a target protein. As we have described, enzymes with a shallowly buried N-terminal amide can be identified through crystal structure or homologous modeling. Whether the immobilization of other enzymes on commonly used carriers can benefit from the extension of tags, such as poly-His, remains uncertain, and further experiments are being conducted in our lab.

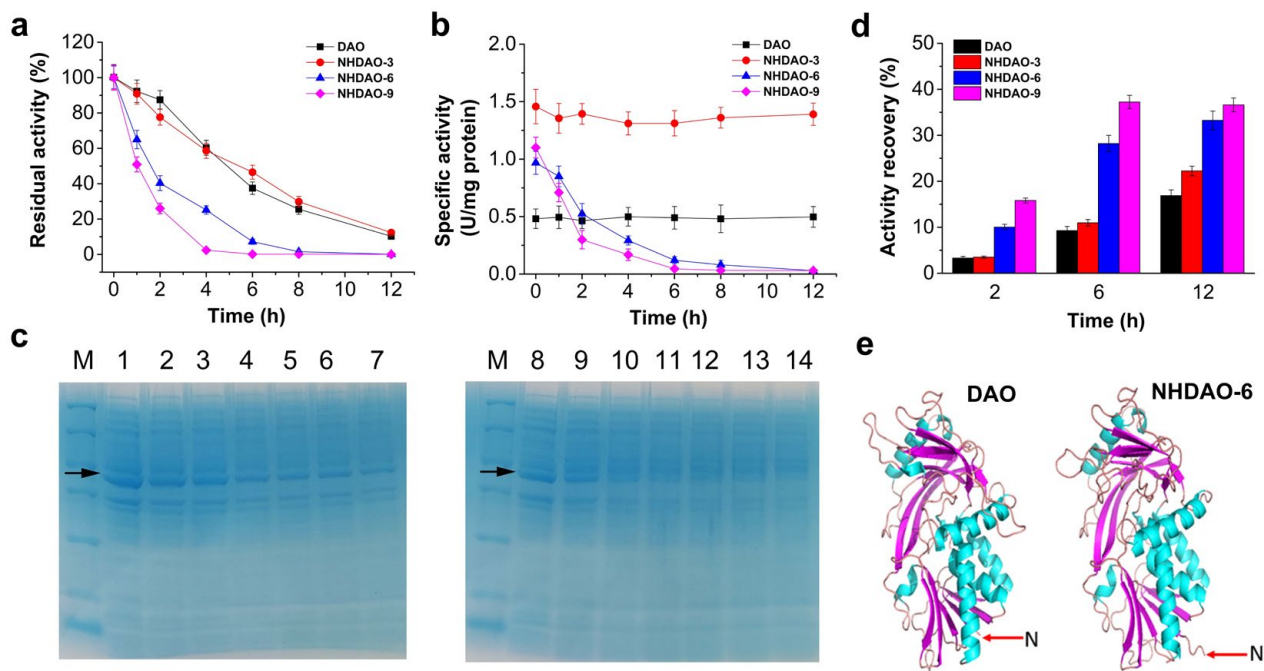


**Figure 3.** Effects of His-tag lengths on DAO immobilization. (a) Residual activity of the supernatants during the immobilization process. (b) Specific activity of the supernatants during the immobilization process. Square (■), DAO. Circle (●), NHDAO-3. Upper triangle (▲), NHDAO-6. Rhombus (◆), NHDAO-9. (c) SDS-PAGE analysis of the supernatants at different time points. Lanes 1, 2, 3, 4, 5, 6, and 7 are the supernatants of DAO at 0 h, 1 h, 2 h, 4 h, 6 h, 8 h, and 12 h. Lanes 8, 9, 10, 11, 12, 13, and 14 are the supernatants of NHDAO-9 at 0 h, 1 h, 2 h, 4 h, 6 h, 8 h, and 12 h. Lane M: protein molecular marker of, from top to bottom, 116, 66.2, 45, 35, 25, 18.4, and 14.4 kDa. The arrow indicates the bands corresponding to DAOs. (d) Rates of activity recovery of immobilized DAOs at 2 h, 6 h, and 12 h. The error bars represent the SDs of three independent experiments. (e) Structure of the homology models of DAO and NHDAO-6. The  $\alpha$ -helix is represented by blue spirals,  $\beta$ -sheet is represented by purple arrows, and light brown ribbons are others. The arrow indicates the N-terminus of DAO.

#### 4. Conclusions

In conclusion, this study primarily demonstrated the soluble expression and rapid, selective immobilization of DAO from *Trigonopsis variabilis* by modulating the length of His-tags. Specifically, the use of a His6 tag enables the soluble expression of recombinant DAO, while the balance between cell growth and protein solubility can be obtained by His3-tag fusion, resulting in a higher activity. However, further research is still required to determine the optimal strain at the fermentor level. Interestingly, longer His-tags facilitate the selective immobilization of DAO on commercial carriers due to their higher immobilization rate. This process is time-saving and cost-effective compared with previous reports using expensive heterofunctional carriers. These findings provide valuable insights for optimizing the use of His-tags in enzyme expression and immobilization. Further research is necessary to determine the effects of His-tag length on the catalytic performance of immobilized DAO.

**Author Contributions:** S.D. and E.M. conceived the idea for the project and wrote the paper. Z.Y., Q.Z., L.M. and G.L. conducted most of the experiments. E.S., J.Z. and Y.C. analyzed the results. All authors have read and agreed to the published version of the manuscript.

**Funding:** This research was funded as a scientific research project by the Education Department of Hunan Province of China, grant number (21B0459). Open fund was also provided by the Hunan Key Laboratory of Economic Crops Genetic Improvement and Integrated Utilization, grant number (E22214).

**Institutional Review Board Statement:** This article does not contain any studies with human participants or animals performed by any of the authors.

**Data Availability Statement:** The data that support the findings of this study are available from the corresponding author upon reasonable request.

**Conflicts of Interest:** The authors declare that they have no conflict of interest.

## References

1. Porath, J.; Carlsson, J.; Belfrage, G.; Olsson, I. Metal chelate affinity chromatography, a new approach to protein fractionation. *Nature* **1975**, *258*, 598–599. [[CrossRef](#)] [[PubMed](#)]
2. Wingfield, P.T. Overview of the purification of recombinant proteins. *Curr. Protoc. Protein Sci.* **2015**, *80*, 6.1.1–6.1.35. [[CrossRef](#)] [[PubMed](#)]
3. Loughran, S.T.; Bree, R.T.; Walls, D. Purification of Polyhistidine-Tagged Proteins. In *Protein Chromatography Methods in Molecular Biology*; Walls, D., Loughran, S., Eds.; Humana Press: New York, NY, USA, 2017; Volume 1485, pp. 275–303.
4. Deng, S.; Zhu, S.; Zhang, X.; Sun, X.; Ma, X.; Su, E. High-level expression of nitrile hydratase in *Escherichia coli* for 2-amino-2,3-dimethylbutyramide synthesis. *Processes* **2022**, *10*, 544. [[CrossRef](#)]
5. Deng, S.; Su, E.; Ma, X.; Yang, S.; Wei, D. High-level soluble and functional expression of *Trigonopsis variabilis* D-amino acid oxidase in *Escherichia coli*. *Bioprocess. Biosyst. Eng.* **2014**, *37*, 1517–1526. [[CrossRef](#)] [[PubMed](#)]
6. Woestenenk, E.A.; Hammarström, M.; van den Berg, S.; Härd, T.; Berglund, H. His tag effect on solubility of human proteins produced in *Escherichia coli*: A comparison between four expression vectors. *J. Struct. Funct. Genom.* **2004**, *5*, 217–229. [[CrossRef](#)] [[PubMed](#)]
7. Gaberc-Porekar, V.; Menart, V. Potential for using histidine tags in purification of proteins at large scale. *Chem. Eng. Technol.* **2005**, *28*, 1306–1314. [[CrossRef](#)]
8. Knecht, S.; Ricklin, D.; Eberle, A.N.; Ernst, B. Oligohis-tags: Mechanisms of binding to Ni<sup>2+</sup>-NTA surfaces. *J. Mol. Recognit.* **2009**, *22*, 270–279. [[CrossRef](#)]
9. Mohanty, A.K.; Wiener, M.C. Membrane protein expression and production: Effects of polyhistidine tag length and position. *Protein Expr. Purif.* **2004**, *33*, 311–325. [[CrossRef](#)]
10. Köppl, C.; Lingg, N.; Fischer, A.; Kröß, C.; Loibl, J.; Buchinger, W.; Schneider, R.; Jungbauer, A.; Striedner, G.; Cserjan-Puschmann, M. Fusion Tag Design Influences Soluble Recombinant Protein Production in *Escherichia coli*. *Int. J. Mol. Sci.* **2022**, *23*, 7678. [[CrossRef](#)]
11. Sheldon, R.A. Enzyme immobilization: The quest for optimum performance. *Adv. Synth. Catal.* **2007**, *349*, 1289–1307. [[CrossRef](#)]
12. Deng, S.; Ma, X.; Sun, M.; Wei, D.; Su, E. Efficient enzymatic synthesis of ampicillin using mutant penicillin G acylase with bio-based solvent glycerol. *Catal. Commun.* **2016**, *79*, 31–34. [[CrossRef](#)]
13. Deng, S.; Ma, X.; Su, E.; Wei, D. Efficient cascade synthesis of ampicillin from penicillin G potassium salt using wild and mutant penicillin G acylase from *Alcaligenes faecalis*. *J. Biotechnol.* **2016**, *219*, 142–148. [[CrossRef](#)]
14. Rodrigues, R.C.; Berenguer-Murcia, Á.; Carballares, D.; Morellon-Sterling, R.; Fernandez-Lafuente, R. Stabilization of enzymes via immobilization: Multipoint covalent attachment and other stabilization strategies. *Biotechnol. Adv.* **2021**, *52*, 107821. [[CrossRef](#)]
15. dos Santos, J.C.S.; Barbosa, O.; Ortiz, C.; Berenguer-Murcia, A.; Rodrigues, R.C.; Fernandez-Lafuente, R. Importance of the support properties for immobilization or purification of enzymes. *ChemCatChem* **2015**, *7*, 2413–2432. [[CrossRef](#)]
16. Luo, M.; Zhang, M.; Chen, G.; Zhao, J.; Guo, H. A potential method for one-step purification and direct immobilization of target protein in cell lysate with magnetic microbeads. *Biochem. Eng. J.* **2021**, *176*, 108182. [[CrossRef](#)]
17. Freitas, A.I.; Domingues, L.; Aguiar, T.Q. Tag-mediated single-step purification and immobilization of recombinant proteins toward protein-engineered advanced materials. *J. Adv. Res.* **2021**, *36*, 249–264. [[CrossRef](#)]
18. Magnusdottir, A.; Johansson, I.; Dahlgren, L.G.; Nordlund, P.; Berglund, H. Enabling IMAC purification of low abundance recombinant proteins from *E. coli* lysates. *Nat. Methods* **2009**, *6*, 477–478. [[CrossRef](#)] [[PubMed](#)]
19. Barbosa, O.; Ortiz, C.; Berenguer-Murcia, Á.; Torres, R.; Rodrigues, R.C.; Fernandez-Lafuente, R. Strategies for the one-step immobilization–purification of enzymes as industrial biocatalysts. *Biotechnol. Adv.* **2015**, *33*, 435–456. [[CrossRef](#)]
20. Bradford, M.M. A rapid and sensitive method for the quantitation of microgram quantities of protein utilizing the principle of protein-dye binding. *Anal. Biochem.* **1976**, *72*, 248–254. [[CrossRef](#)]
21. Ma, X.; Deng, S.; Su, E.; Wei, D. One-pot enzymatic production of deacetyl-7-aminocephalosporanic acid from cephalosporin C via immobilized cephalosporin C acylase and deacetylase. *Biochem. Eng. J.* **2015**, *95*, 1–8. [[CrossRef](#)]
22. Yang, J.; Zhang, Y. I-TASSER server: New development for protein structure and function predictions. *Nucleic Acids Res.* **2015**, *43*, 174–181. [[CrossRef](#)] [[PubMed](#)]
23. Wong, K.S.; Fong, W.P.; Tsang, P.W. A single Phe<sup>54</sup>Tyr substitution improves the catalytic activity and thermostability of *Trigonopsis variabilis* D-amino acid oxidase. *New Biotechnol.* **2010**, *27*, 78–84. [[CrossRef](#)]
24. Xu, J.M.; Cao, H.T.; Wang, M.; Ma, B.J.; Wang, L.Y.; Zhang, K.; Cheng, F.; Xue, Y.P.; Zheng, Y.G. Development of a combination fermentation strategy to simultaneously increase biomass and enzyme activity of D-amino acid oxidase expressed in *Escherichia coli*. *Appl. Biochem. Biotechnol.* **2021**, *193*, 2029–2042. [[CrossRef](#)] [[PubMed](#)]

25. Walls, D.; Loughran, S.T. Tagging recombinant proteins to enhance solubility and aid purification. *Methods Mol. Biol.* **2011**, *681*, 151–175.
26. Mateo, C.; Abian, O.; Bernedo, M.; Cuenca, E.; Fuentes, M.; Fernandez-Lorente, G.; Palomo, J.M.; Grazu, V.; Pessela, B.C.C.; Giacomini, C.; et al. Some special features of glyoxyl supports to immobilize proteins. *Enzyme Microb. Technol.* **2005**, *37*, 456–462. [[CrossRef](#)]
27. Garcia-Galan, C.; Berenguer-Murcia, Á.; Fernandez-Lafuente, R.; Rodrigues, R.C. Potential of different enzyme immobilization strategies to improve enzyme performance. *Adv. Synth. Catal.* **2011**, *353*, 2885–2904. [[CrossRef](#)]

**Disclaimer/Publisher’s Note:** The statements, opinions and data contained in all publications are solely those of the individual author(s) and contributor(s) and not of MDPI and/or the editor(s). MDPI and/or the editor(s) disclaim responsibility for any injury to people or property resulting from any ideas, methods, instructions or products referred to in the content.